

## Collision of viscoelastic jets and the formation of fluid webs

Erik Miller, Beau Gibson, Erik McWilliams, and Jonathan P. Rothstein<sup>a)</sup>

*Department of Mechanical and Industrial Engineering, University of Massachusetts, Amherst, Massachusetts, 01003-9265*

(Received 18 February 2005; accepted 26 May 2005; published online 27 June 2005)

This letter reports experimental observations of the flow kinematics and stability of thin fluid sheets produced by impinging obliquely aligned laminar jets of a series of viscoelastic worm-like micelle solutions. As the velocity of the impinging jets is increased, the sheets of viscoelastic fluid grow larger and eventually become unstable. High speed imaging reveals a transition to a striking new flow structure resembling fluid webs, previously unobserved for Newtonian or non-Newtonian fluids. These newly discovered flow structures are complex and comprised of highly interconnected filaments created by the growth of multiple internal failures within the fluid sheet. Increasing viscoelasticity of the test fluid was found to stabilize the sheets and the fluid webs while increasing the drop size produced by their eventual breakup under capillary stresses. © 2005 American Institute of Physics. [DOI: 10.1063/1.1984099]

In this letter, we present the results of an experimental investigation into the collision and subsequent atomization of viscoelastic jets. The impact of fluid jets at an oblique angle is an effective means of generating thin sheets of the colliding fluids.<sup>1,2</sup> The structure, kinematics and stability of thin films has been well studied both experimentally and analytically throughout the literature for Newtonian fluids.<sup>1,3-5</sup> However, despite the importance of these fluids and flows to a host of commercial and industrial applications such as agrochemical spraying, spray coating, and ink jet printing, little work has been done to study the breakup of thin films of viscoelastic fluids.<sup>6-9</sup> The studies that do exist focus primarily on correlating atomization characteristics and droplet size distribution measurements to changes in polymer concentration, molecular weight and fluid rheology. These correlations are often valid only for a specific nozzle design. The mechanisms of breakup in these systems are still not well understood.

A good deal of literature does, however, exist describing the role of viscoelasticity on forestalling the breakup of laminar capillary jets.<sup>10</sup> The breakup dynamics of liquid jets are governed by the extensional viscosity,  $\eta_E$ , and the surface tension,  $\sigma$ , of the fluid. For polymeric or worm-like micelle solutions, the shear and extensional viscosities can be strong functions of the flow kinematics, the rate of deformation and the deformation history,  $\eta=f(\dot{\gamma}, \gamma, t)$ . The dynamical response of the fluids in extensional flows is quite different than in simple shear. Whereas the shear viscosity will often become heavily thin with increasing shear rate, the extensional viscosity can increase by several orders of magnitude with increasing strain.<sup>11</sup> This strain hardening has been shown to stabilize viscoelastic jets while retarding satellite drop formation and increasing the main droplet size.<sup>10,12,13</sup>

To generate the fluid sheets, fluid was pumped through two opposed nozzles set 1.5 cm apart and at an angle of  $\beta=30^\circ$  from the vertical. Velocities up to  $U=10$  m/s were achieved using two identical syringes driven by a linear stepper motor. The inner radius of the nozzles was fixed at

$R=1.5$  mm. Care was taken to insure precise alignment of the nozzles such that the centerlines of the impinging jets intersected, producing a symmetric thin film. Images of the thin films were taken with both a digital single lens reflex (SLR) camera (Nikon D70) with exposure times of 1/4000th of a second and a high speed digital video camera (Phantom V4.2) capable of capturing video at 90 000 frames/s.

A series of viscoelastic worm-like micelle solutions containing between 10 and 25 mM cetyltrimethylammonium bromide (CTAB) and equal molarities of sodium salicylate (NaSal) in distilled, de-ionized water were used in these experiments. The steady shear rheology of these worm-like micelle solutions was found to shear thin very heavily with increasing shear rate<sup>14</sup> while the transient extensional viscosity increased by several orders of magnitude with increasing accumulated Hencky strain.<sup>11</sup> For the sake of completeness, the important rheological parameters of each solution are presented in Table I, and a complete discussion of the fluid rheology can be found in our recent publications.<sup>11,14</sup> For comparison, a Newtonian solution of 65% glycerin and 35% water with constant viscosity of  $\mu=0.015$  Pa s was also used.

In the case of colliding Newtonian jets, the resulting fluid dynamics are controlled by a balance of inertial, gravitational and capillary stresses. At sufficiently high speeds and Reynolds numbers, as is the case for all experiments presented in this letter, the effects of gravity can be neglected. When the fluid is viscoelastic, elastic stresses must also be considered, resulting in changes to both the kinematics and stability of the thin film. The colliding jets produce a flow radially outward within the plane of impact. Surface tension and elasticity resist the spread of the thin film and ultimately restrict its size resulting in the formation of a relatively thick

TABLE I. Parameters characterizing the rheology of the CTAB and NaSal worm-like micelle solutions.

CTAB [mM]	NaSal [mM]	$\eta_0$ [Pa s]	$\lambda$ [s]
10	10	5.0	18
17.5	17.5	41	35
25	25	68	27

<sup>a)</sup> Author to whom correspondence should be addressed; electronic mail: rothstein@ecs.umass.edu

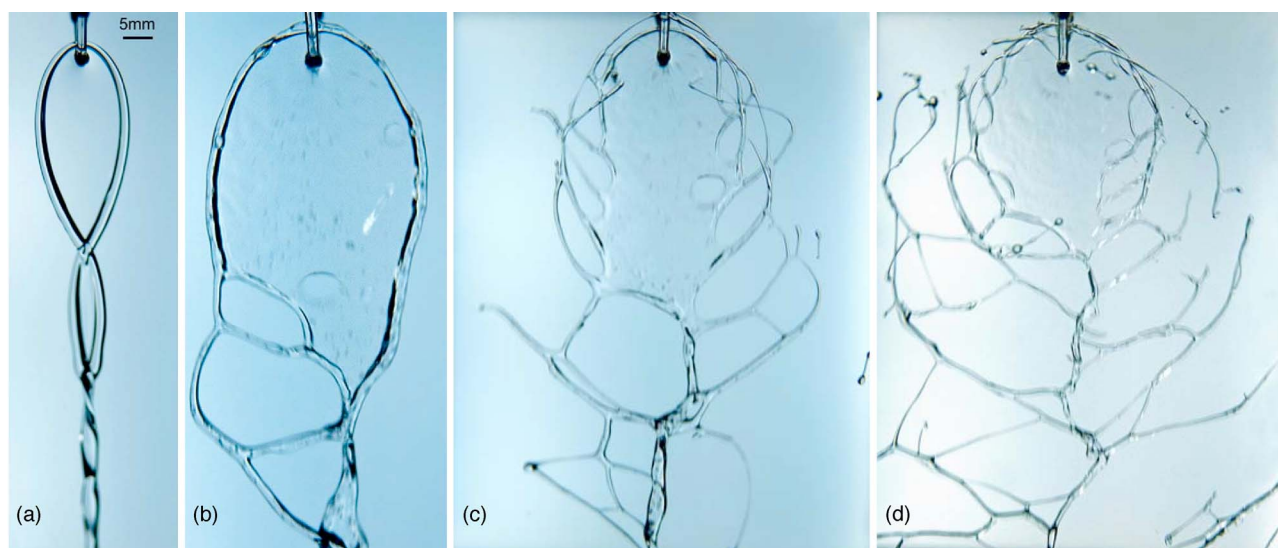


FIG. 1. (Color online) High speed photographs of the fluid sheets formed by impinging jets of (a) 65% glycerin in water at  $U=2.1$  m/s; (b) 17.5 mM CTAB/NaSal at 5.0 m/s; (c) 25 mM CTAB/NaSal at 5.8 m/s; and (d) 25 mM CTAB/NaSal at 6.2 m/s.

rim around the film. The rim eventually closes back on itself forming an apex below the point of impact and giving the sheet a leaf-like appearance. Where the two sides of the rim collide a second thin film is formed normal to the first and so on until the two jets have merged into a single jet.<sup>2</sup> In Fig. 1(a), a cascading fluid chain is shown for the 65% glycerin and water solution. Similar cascades are observed for all of the worm-like micelle solutions, although the links were found to be somewhat less regular and to decay in size significantly faster with each successive link.

As the velocity of the impinging jets is increased, the fluid sheet expands in size and transitions through a series of different flow regimes. Aerodynamic forces or, in some cases, a rim instability<sup>2</sup> are the source of the onset of the initial disturbances in the fluid sheet. Oscillations in the fluid sheet become more pronounced with increasing flow strength. For low viscosity Newtonian fluids such as water these oscillations continue to grow with flow strength resulting in an out-of-plane flapping motion that eventually results in the atomization of the sheet.<sup>1</sup> However, with more viscous Newtonian fluids, fingers appear along the rim producing a flow structure that Bush and Hasha described as fluid “fishbones”.<sup>2</sup> Although oscillations were observed within the rim of the fluid sheet, the increased viscosity and the elasticity of the micelle solutions reduced their amplitude to the point that no fluid fishbones were observed. The viscoelasticity of these fluids did, however, result in a series of previously unobserved flow phenomena and flow stability transitions. This lack of fluid fishbones is consistent with the findings of Bush and Hasha who found that fishbones exist in a very narrow Reynolds number range,  $250 \leq Re \leq 1200$ . The Reynolds numbers in our viscoelastic fluids experiments were all less than one,  $Re = \rho UR / \eta_0 < 1$ . Here  $\eta_0$  is the zero shear rate viscosity.

Above a critical flow rate, the sheets experience a randomly located internal failure, as if pricked by a pin. As the capillary and elastic stresses retract the sheet from the rapidly expanding hole, an internal rim is formed. Several stages of growth can be clearly seen in Fig. 1(b). As the flow rate is increased, the frequency of these rupture events also increases. As seen in Fig. 1(c), the rims produced by multiple

rupture events will eventually collide to produce a complicated interconnected, planar structure which we will refer to as “fluid webs.” At still larger jet velocities, some filaments break or detach from the web to form “fluid tendrils.” These tendrils can be seen clearly in Fig. 1(d) and are often formed through capillary driven pinch-off of the fluid filament. The Ohnesorge number in the fluid filaments is greater than  $Oh = \eta_0 / \sqrt{\rho \sigma R} > 50$ . For a Newtonian fluid in this high Ohnesorge number regime the time scale for breakup is given by  $t_R = \sqrt{\rho R^3 / \sigma}$ . However, for a viscoelastic fluid, the breakup is governed by the relaxation time of the fluid,  $\lambda$ . The ratio of these time scales is a natural or intrinsic Deborah number which for all of our experiments was very large,  $De_0 = \lambda \sqrt{\sigma / \rho R^3} \gg 1$ . Thus elasticity forestalls breakup of the fluid filaments. Occasionally, the sheet ruptures above the intersection point of the impinging jets, and the resulting out-of-plane motion of the rim causes it to be dissected as it passes through the stream of one of the impinging jets. The curious reader is referred to the author’s web site to view

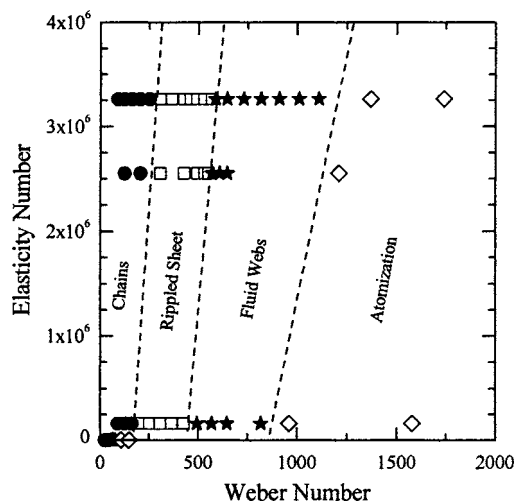


FIG. 2. Diagram illustrating the dependence of the stability and structure of the rim on flow strength and fluid rheology. Borders between the flow regime are not intended to be quantitative, but are meant only to guide the reader’s eye.

high speed movies of these breakup events.<sup>15</sup>

The progression of the flow structures, shown in Fig. 2, is mapped out in a diagram showing the dependence of the structure on the governing dimensionless groups, the elasticity number which is a ratio of the Weissenberg and Reynolds numbers,  $El = Wi/Re = \lambda \eta_0 / \rho R^2$ , and the Weber number,  $We = \rho U^2 D / \sigma$ . Of course these dimensionless groups represent a slice in a multidimensional parameter space containing all the possible dimensionless groups. The figure clearly shows that increasing the elasticity forestalls each of the identifiable flow transitions. The large extensional viscosities of these micelle solutions retard the breakup of the interconnected fluid filaments making the fluid webs remarkably long lived. These experiments suggest that if a volatile solvent were used, polymeric webs could be generated from solution if enough solvent could be evaporated to solidify the polymeric solution before the filaments break up.<sup>16</sup> In addition, a quantitative analysis of our high speed images shows that for a fixed Weber number, the aspect ratio of the initial fluid sheet decreases and the diameter of satellite drops produced by atomization of the thin film increase substantially with increasing fluid elasticity.

- <sup>1</sup>N. Dombrowski and R. P. Fraser, *Philos. Trans. R. Soc. London, Ser. A* **247**, 101 (1954).
- <sup>2</sup>J. W. M. Bush and A. E. Hasha, *J. Fluid Mech.* **511**, 285 (2004).
- <sup>3</sup>C. J. Clark and N. Dombrowski, *Proc. R. Soc. London, Ser. A* **329**, 467 (1972).
- <sup>4</sup>Y.-J. Choo and B.-S. Kang, *Phys. Fluids* **14**, 622 (2002).
- <sup>5</sup>G. I. Taylor, *Proc. R. Soc. London, Ser. A* **253**, 313 (1959).
- <sup>6</sup>L.-L. Xing and J. E. Glass, *J. Coat. Technol.* **71**, 3750 (1999).
- <sup>7</sup>R. P. Mun, B. W. Young, and D. V. Boger, *J. Non-Newtonian Fluid Mech.* **83**, 163 (1999).
- <sup>8</sup>M. Stelter, G. Brenn, and F. Durst, *Atomization Sprays* **12**, 299 (2002).
- <sup>9</sup>G. M. Harrison, R. P. Mun, G. Cooper, and D. V. Boger, *J. Non-Newtonian Fluid Mech.* **85**, 93 (1999).
- <sup>10</sup>R. P. Mun, J. A. Byers, and D. V. Boger, *J. Non-Newtonian Fluid Mech.* **74**, 285 (1998).
- <sup>11</sup>J. P. Rothstein, *J. Rheol.* **47**, 1227 (2003).
- <sup>12</sup>H. A. Stone, *Annu. Rev. Fluid Mech.* **26**, 65 (1994).
- <sup>13</sup>M. Renardy, *J. Non-Newtonian Fluid Mech.* **59**, 267 (1995).
- <sup>14</sup>J. Lampe, R. DiLalla, J. Grimaldi, and J. P. Rothstein, *J. Non-Newtonian Fluid Mech.* **125**, 11 (2005).
- <sup>15</sup>[http://www.ecs.umass.edu/mie/faculty/rothstein/active\\_res.htm#webs](http://www.ecs.umass.edu/mie/faculty/rothstein/active_res.htm#webs)
- <sup>16</sup>A. Tripathi, P. Whitingstall, and G. H. McKinley, *Rheol. Acta* **39**, 321 (2000).